ELSEVIER

Catalysis Today 81 (2003) 659–671

CATALYSIS TODAY

www.elsevier.com/locate/cattod

Deactivation and regeneration of Pt/γ-alumina and Pt/ceria–alumina catalysts for methane combustion in the presence of H_2S

D.J. Fullerton [a], A.V.K. Westwood [a], R. Brydson [b], M.V. Twigg [c], J.M. Jones [a,*]

[a] *Department of Fuel & Energy, SPEME, University of Leeds, Leeds LS2 9JT, UK*
[b] *Department of Materials, SPEME, University of Leeds, Leeds LS2 9JT, UK*
[c] *Johnson Matthey, Catalytic Systems Division, Orchard Road, Royston, Herts. SG8 5HE, UK*

Abstract

Ceria has been widely explored as an additive in alumina-supported precious metal catalysts due to a number of unique properties. The success of ceria and ceria-based materials is mainly attributed to the unique combination of an elevated oxygen transport capacity coupled with the ability to shift easily between reduced and oxidised sates. In this study the influence of CeO_2 addition to a Pt/Al_2O_3 catalyst for low temperature (<540 °C) methane oxidation in an oxidising environment has been investigated. The resistance to H_2S-poisoning and influence on catalyst regeneration by oxidation or reductive treatments has been studied. The addition of CeO_2 to the support creates an increase in the level of activity based primarily on the oxygen storage capacity offered by the cerium oxide, causing an increase in oxygen activation. The ceria–alumina-supported catalyst showed a greater shift to poorer activity upon exposure to H_2S. It appears sulphur compounds react with the oxygen storage component causing a decrease in oxygen transfer, removing any benefit offered by the ceria. However, the level of Pt-agglomeration and support changes were reduced with the incorporation of ceria, emphasising the stabilising effect and promotion of metal particle dispersion associated with ceria. In order to obtain the maximum benefit of ceria addition to the support structure in terms of activity a reductive pretreatment is required. Upon exposure to a reducing atmosphere, it appears a Pt–CeO_2 interaction generates greater levels of activity.

Keywords: Platinum; Alumina; Ceria; Sulphur; Catalyst poisoning; Regeneration

1. Introduction

Gas turbines are being increasingly used for electric power generation and other applications because they are efficient and clean burning. However, without emissions controls they emit more nitrogen oxides (NO_X) than regulations permit. Commercial NO_X control techniques, such as dry low NO_X, wet diluent injection, and selective catalytic reduction, are generally uneconomical for achieving NO_X emissions of 10 ppm or less, which are, or will soon be required in many industrialised regions of the world. In the thermal combustion of natural gas, NO_X emissions are very low up to about 1400 °C, but increase sharply to more than 160 ppm at the typical flame temperature of about 1800 °C. In catalytic combustion, which occurs

* Corresponding author. Tel.: +44-113-343-2477; fax: +44-113-246-7310.
E-mail address: j.m.jones@leeds.ac.uk (J.M. Jones).

0920-5861/03/$ – see front matter © 2003 Elsevier B.V. All rights reserved.
doi:10.1016/S0920-5861(03)00164-0

at 1300–1400 °C, NO_X emissions can be as low as 2–5 ppm [1]. Thus, from the environmental point of view, catalytic combustion is an attractive way to produce thermal energy of high quality, since it allows efficient and complete burning at temperatures lower than in flame combustion and without yielding undesired by-products.

Some concepts have been proposed to attain ideal catalytic combustion for high temperature applications such as gas turbines. For practical applications, two kinds of catalyst materials are required: one having high catalytic activity with a low ignition temperature, and the other possessing high heat resistance, good catalytic activity, surface area, and thermal shock resistance. For high temperature performance, some hexaaluminate compounds used in the multi-monolith reactor are the most promising catalysts as they are heat resistant materials with a moderate catalytic activity. On the other hand, platinum group metal catalysts (e.g. Pd/Pt/Rh) are the most active ignition catalysts [2–7]. Higher catalytic activity per site and greater resistance to sulphur poisoning (below 773 K) are the main advantages of precious metal catalysts over metal-oxide catalysts [4,8].

Platinum group metal catalysts can be used either with or without a support, but supported metal catalysts are favoured for the oxidation. Among the advantages of supported metal catalysts is that the metal is dispersed over a greater surface area of the support and shows different activity from the unsupported metals due to interactions of the metal with the support. The support acts to stabilise thermally the catalyst and, in some cases, may be involved in the catalytic reaction. In general, catalytic combustors use a washcoated monolith to obtain high geometric areas for good heat/mass transfer and low pressure drop through the system. The washcoat, commonly γ-Al_2O_3, is coated on the substrate to provide a high surface area. However, above 1000 °C, the high surface area γ-Al_2O_3 changes to relatively low surface area α-Al_2O_3 [8]. Addition of ceria (CeO_2) to these supports has aimed to physically inhibit changes to the structure of the γ-Al_2O_3 and thus maintain good dispersion and activity of the metal catalyst at high temperatures and/or during thermal cycling [9–14].

Cerium oxide can store and/or release reversibly a large amount of oxygen, responding to the gas-phase oxygen concentration [9,11,12,15–17]. Consequently, cerium oxide has been employed as a base component of automobile three-way catalysts in order to control pollutant emissions. In addition, CeO_2 is a well-known promoter in precious metal combustion catalysts. Particularly, the presence of CeO_2 has been found effective in the promotion of various catalytic reactions including, CO_2 activation, CO oxidation and CO/NO removal [9,17,18]. For the catalytic combustion of methane, the support plays an important part in determining the activity and long-term stability of the catalysts. These effects have been investigated in some detail. However, research into ceria–alumina-supported platinum group metals for catalysed low temperature methane combustion has been mainly confined to studies using palladium [5,12,15,16,18,19–21]. The few studies carried out using platinum have generated conflicting results.

Several studies have reported that the presence of CeO_2 can improve the CO total oxidation activity of pre-reduced precious metal catalysts [22–28]. For example, Oh and Eickel [24] reported that CO self-inhibition was suppressed by the addition of cerium oxides to Pt/Al_2O_3 catalyst during CO oxidation under moderately oxidising or net-reducing conditions. Summers and Ausen [22] reported similar results that the CO oxidation activity of Pt/Al_2O_3 was enhanced upon the addition of small quantities of cerium oxides, yielding partially oxidised metals. However, under oxidising conditions it has been reported that $Pt/CeO_2/Al_2O_3$ catalysts are less active than corresponding Pt/Al_2O_3 samples for the oxidation of alkanes [29–34]. This was attributed to increased oxidation of surface Pt sites in the presence of CeO_2, or to an improved dispersion of Pt particles preventing the formation of larger metallic particles necessary for hydrocarbon oxidation. For example, Yu-Yao [30] and Oh et al. [34] reported the addition of cerium oxide depressed the activity of alumina-supported precious metal catalysts for methane oxidation. It was suggested that transformation of precious metals from a more active species to a less active species occurs as a result of active oxygen species formed on cerium oxide. Similarly, Kummer et al. [33] reported that for alkane oxidations on Pt/Al_2O_3 the catalytic activity decreased with the addition of cerium oxides because of the formation of surface-oxidised platinum.

The potential of CeO_2 to oxidise hydrocarbons has been known for several years and is found to be strongly dependent on pretreatment atmosphere and temperature [17]. The effect of reductive pretreatments on the hydrocarbon oxidation activity of cerium oxide containing platinum group metal catalysts has been investigated in previous studies [27–30,32]. Under reducing conditions Engler et al. [27] reported, the presence of CeO_2 had a strong positive effect on CO activity but hydrocarbon conversions were highest on monometallic Pt/Al_2O_3. Yu-Yao [30] found that the CO combustion activity of reduced $Pt/CeO_2/Al_2O_3$ catalysts was considerably greater than that of unreduced Pt/Al_2O_3 or $Pt/CeO_2/Al_2O_3$ samples at equivalent Pt loadings under O_2-rich conditions. A recent study by Tiernan using $Pt/CeO_2/Al_2O_3$ involves the combustion of *iso*-butane. Catalysts containing higher levels of ceria, i.e. Ce:Pt > 8:1, initially showed poorer activities in the combustion of *iso*-butane than Pt/Al_2O_3. However, after reduction of the catalysts this effect was reversed and highest overall activities were obtained after reduction of the $Pt/CeO_2/Al_2O_3$ catalysts. This has been explained in terms of a bimetallic surface interaction in which ceria decreases catalyst surface reducibility [11].

Poisoning by sulphur compounds, such as H_2S is encountered in many large-scale processes using metal catalysts, such as methanation, steam reforming and hydrogenations. Natural gas may contain traces of sulphur in which it usually exists as H_2S. The adverse impact of sulphur compounds on catalytic performance is well known [8,35–41]. The loss of catalyst activity during sulphur poisoning of Pt/Al_2O_3 has been attributed to the adsorption of H_2S, sulphur-poisoning-induced Pt-agglomeration and the formation of platinum sulphides [41]. These interactions, besides causing a decrease in the catalytic conversion, may also exert some positive effects. In fact, if the catalyst is passivated with the poison, a significant enhancement in the selectivity may be produced. An increase in the activity of Pt/Al_2O_3 catalysts in dehydrogenation has been reported, which was attributed to different sulphur–metal interactions depending upon the platinum salt used in the catalyst preparation [42]. A similar enhancement in the activity of Pt/Al_2O_3 by H_2S in the catalytic combustion of methane has also been reported [8]. Also, sulphur trioxide is reported to react with components of the washcoat to increase the oxidation activity of platinum [43].

H_2S may also be catalytically oxidised to SO_2 and then to SO_3 which can react with the support to form sulphates. The interaction of SO_2 with a reducible oxide under changing redox conditions can be complex. In addition to undergoing chemisorption, SO_2 has been reported to act either as a reductant or as an oxidant on ceria [44,45]. A study by Lööf et al. [25] showed the presence of trivalent sulphate after exposing a 3 wt.% Pt/CeO_2 catalyst to 2% SO_2, 5% O_2 in N_2 at 500 °C. A bulk sulphating process was proposed in contrast to the SO_2 exposed Al_2O_3 catalyst which showed only surface sulphation. Using two different ceria samples Waqif showed that the relative amount of each type of sulphate species (bulk-like and surface) and the temperature of their formation depends on the texture of the samples [45]. Both types begin to decompose by heating at 600 °C, but some surface species are still adsorbed at 700 °C showing that their thermal stability is close to that found for sulphates on ZrO_2. Heating under H_2 at a temperature higher than 500 °C leads to the reduction of all sulphates. Such a reduction temperature is relatively low when compared to other oxides. This could be due to the redox properties of ceria. Under certain conditions, ceria, due to its ability to store and release sulphur, has been shown to increase the negative impact of sulphur [46]. In a more recent study, it was shown that small amounts of SO_2 have a dramatic effect on the catalytic properties of ceria-supported platinum group metals, primarily by interacting with ceria [47]. For pre-exposure of 20 ppm SO_2 at 673 K, no changes in light-off curves for CO oxidation on Pd/Al_2O_3 was observed. The same pre-exposure of SO_2 to $Pd/CeO_2/Al_2O_3$ resulted in a significant upward shift in the light-off curve.

Clearly CeO_2 can promote or inhibit the metal catalysed oxidation reaction because of the influence on the metal species present under different gaseous environments. One of the aims of the present study is to examine the influence of CeO_2 on low temperature (<540 °C) methane oxidation in an oxidising environment. It also seeks to investigate the effect of a reductive treatment on the catalyst activity. A third aim of this work is to compare catalyst deactivation via S-poisoning of both γ-Al_2O_3 and CeO_2/Al_2O_3 supported Pt catalysts, and to explore catalyst regeneration after poisoning.

2. Experimental

2.1. Catalyst preparation

The catalysts used in the experiments were provided by Johnson Matthey. The two catalysts tested were 3.79 wt.% Pt/Al_2O_3 and 3.79 wt.% Pt/12% CeO_2/Al_2O_3. The catalysts were calcined in air at 475 °C for 4 h at 4 °C/min. The surface areas of the calcined catalysts were determined by the BET method using a Quantasorb surface area analyser.

2.2. Activity in the catalytic combustion of methane

Approximately 100 mg, accurately weighed, of each powdered catalyst, sieved to ≤150 μm, was pretreated by a further 30 min treatment in air at 475 °C (60 ml/min) in situ on a horizontal cross-sectional glass frit in a vertical tubular silica micro-reactor at atmospheric pressure. Conversion to CO_2 over a range of temperatures, of a 100 ml/min gas feed consisting of air (40 ml/min), nitrogen (56.4 ml/min), methane (3.6 ml/min) and hydrogen sulphide (2.4 ml/h when applicable) was monitored using on-line gas chromatography. A Perkin Elmer Autosystem XL gas chromatograph fitted with an Alltech CTR 1 column in series with thermal conductivity and flame ionisation detectors was used to detect CH_4, O_2 and CO_2 in the feed and flue gases. Although this system was also capable of measuring CO concentrations this gas was not detected in any of the experiments. All gas concentrations were calibrated against standard gas mixtures. For each catalyst, conversion vs. temperature was monitored when (i) freshly pretreated in air, (ii) poisoned with 30 ppm H_2S, (iii) regenerated in air (30 min in 60 ml/min air at 475 °C), (iv) regenerated in H_2 (30 min in 60 ml/min H_2 at 475 °C). In the catalytic activity measurements, the temperatures quoted all refer to bed temperatures. The reproducibility of the methane conversion has a relative error of ±3%.

2.3. Transmission electron microscope (TEM)

TEM examination was carried out with a Phillips FEI CM200 FEG TEM fitted with a Gatan imaging filter (GIF). Samples were dispersed in acetone and drop cast onto holey carbon films (Agar). Images were taken of the fresh, poisoned and H_2 regenerated catalyst samples. These images were used to provide particle size measurements and indicate the condition of the catalyst surface structure.

3. Results

The activity–temperature curves are shown in Fig. 1. From the data at <30% conversion, kinetic parameters were derived assuming that the apparent first order mass specific rate constant (k_m) is given by

$$-\left(\frac{F}{m}\right)[\ln(1-x)] = k_m = A\exp\left(-\frac{E_a}{RT}\right)$$

where F/m is the temperature-corrected volumetric rate of methane/air feed divided by the weight of catalyst (i.e. the reciprocal of the space-time divided by a constant, catalyst density). Work by Jones et al. [48] provides a more detailed description of the derivation of the kinetic parameters. The activation energies, E_a, and the pre-exponential factors, A, for the catalytic combustion of methane were estimated from Arrhenius plots. These are summarised in Table 1. As a comparative parameter, the apparent first order rate constants, evaluated at 623 K are also presented in Table 1.

From the results (Fig. 1), it can be seen that the ceria–alumina-supported catalyst is more active for

Table 1
Comparison of the kinetic parameters for both Pt/Al_2O_3 and $Pt/CeO_2/Al_2O_3$

	Pt/Al_2O_3	$Pt/CeO_2/Al_2O_3$	
E_a (kJ mol^{-1})			
Fresh	92 ± 3	89 ± 3	
H_2S poisoned	97 ± 1	70 ± 3	(98 ± 3)
Air regenerated	96 ± 3	101 ± 2	
H_2 regenerated	78 ± 1	81 ± 3	
A (ml s^{-1} g^{-1})			
Fresh	1×10^8	7×10^7	
H_2S poisoned	2×10^8	2×10^6	(2×10^8)
Air regenerated	1×10^8	3×10^8	
H_2 regenerated	7×10^6	5×10^7	
K_{m623} (ml s^{-1} g^{-1})			
Fresh	1.91	2.33	
H_2S poisoned	1.17	2.37	(1.43)
Air regenerated	1.03	0.97	
H_2 regenerated	2.15	8.29	

Numbers in brackets refer to results obtained if data at <6% conversion is neglected.

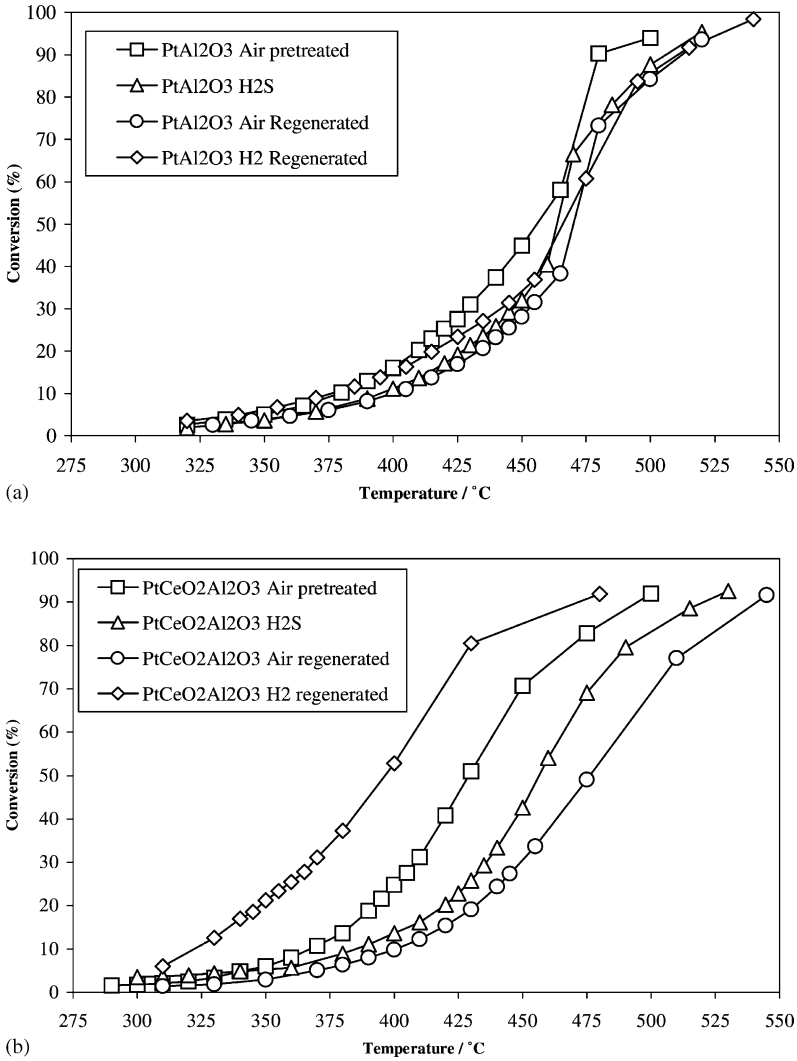

Fig. 1. Conversion vs. temperature curves for catalysed methane combustion over: (a) Pt/Al_2O_3 and (b) $Pt/CeO_2/Al_2O_3$ after various treatments.

low temperature methane combustion. Under identical reaction conditions, a temperature of 460 °C is required to reach 50% conversion for the alumina-supported catalyst in comparison to a temperature of 430 °C recorded for the ceria–alumina-supported analogue. Whilst the ceria–alumina-supported catalyst remained more active upon exposure to the hydrogen sulphide mixture, it was clear that both catalysts suffered a certain level of deactivation through sulphur poisoning. This is manifested as a shift in the temperature–conversion curves to higher temperatures. The shift in temperature for 50% methane conversion is greater for $Pt/CeO_2/Al_2O_3$ compared to Pt/Al_2O_3 but the H_2S has a smaller influence on $Pt/CeO_2/Al_2O_3$ at lower conversions (i.e. lower temperature). In fact, a possible promotional effect of H_2S is seen in conversions below 6%. If all the data below 30% conversion shown in Fig. 1 is used in the kinetic analysis then an activation energy of 70 kJ mol^{-1} is obtained. However, if the data at <6% conversion is neglected then an activation energy of 98 kJ mol^{-1} is obtained, which is consistent with the observed poisoning at higher

temperatures. There is a decrease in k_{m623} for both catalysts upon exposure to the H_2S mixture although more significant in the case of the alumina-supported catalyst, indicating a greater loss in activity.

It can be seen from Fig. 1 and Table 1, that regeneration in air at 475 °C was ineffective and in fact resulted in further catalyst deactivation for both Pt/Al_2O_3 and $Pt/CeO_2/Al_2O_3$. However, reductive regeneration was effective for both catalysts, particularly $Pt/CeO_2/Al_2O_3$, where the catalyst activity surpassed that originally seen for the freshly calcined sample, with a k_{m623} value of 8.29 ml s^{-1} g^{-1}.

In order to compare the relative poison resistance of each catalyst, the performance of the poisoned catalyst was normalised to that of the fresh catalyst used to produce an "activity coefficient". At any given temperature, this coefficient is defined as the difference between the mass specific rate constants for poisoned and fresh systems divided by the mass specific rate constant of the fresh system, i.e.:

$$\text{Poisoned activity coefficient, } p_{AC} = \frac{k_{m(\text{poisoned})} - k_{m(\text{fresh})}}{k_{m(\text{fresh})}}$$

Thus, a large negative value of p_{AC} implies a large degree of poisoning. A similar comparison can be performed to analyse the effectiveness of the regeneration of the poisoned catalysts, i.e.:

$$\text{Regenerated activity coefficient, } r_{AC} = \frac{k_{m(\text{regenerated})} - k_{m(\text{fresh})}}{k_{m(\text{fresh})}}$$

A higher value of r_{AC} implies more successful regeneration. The relative error in the calculated activity coefficients is approximately 4%.

The calculated activity coefficients can be seen summarised in Fig. 2. These results support the earlier observations that although the $Pt/CeO_2/Al_2O_3$ catalyst shows a bigger overall shift in conversion in response to the H_2S, it is much less affected at lower temperatures in comparison to Pt/Al_2O_3, and is in fact promoted at the lower temperatures. It should be remembered that as the temperature is increased, the catalyst has seen an increasing total amount of H_2S, even though the H_2S concentration is constant. The negative activity coefficients resulting from air regeneration illustrates air regeneration was ineffective for both catalysts over the entire temperature range studied. It would appear this process goes further to deactivate the catalysts, particularly in the case of $Pt/CeO_2/Al_2O_3$. This is not the case, however, with reductive regeneration (Fig. 1 and Table 1). Hydrogen regeneration was successful for both catalysts, especially for $Pt/CeO_2/Al_2O_3$. A positive activity coefficient seen in Fig. 2 indicates that the activity upon regeneration is considerably higher than that measured for the freshly calcined catalyst.

From the TEM images (Fig. 3), it was possible to obtain the average metal particle sizes given in Table 2. These were determined using in excess of 30 particle sizes obtained from a series of representative images. Table 2 also gives the BET surface areas of the catalysts after different temperature and pretreatment histories. The metal particle sizes are slightly smaller for Pt/Al_2O_3 when the catalysts were in their fresh calcined states. After a second activity–temperature cycle and in the presence of H_2S, both catalysts displayed increased metal particle size and this agglomeration was most severe for Pt/Al_2O_3. It can be seen (Fig. 3c–f) that in response to the H_2S, the support structure of the Pt/Al_2O_3 catalysts changed quite drastically as opposed to the that of the $Pt/CeO_2/Al_2O_3$ catalyst that remained almost unchanged. The $Pt/CeO_2/Al_2O_3$ catalyst responded better towards reductive redispersion of the metal compared to Pt/Al_2O_3. The regenerated $Pt/CeO_2/Al_2O_3$ catalyst had an average particle diameter which is half the size of the particles of Pt/Al_2O_3.

Table 2
Catalyst characterisation for average particle sizes and surface areas for both Pt/Al_2O_3 and $Pt/CeO_2/Al_2O_3$

	Pt/Al_2O_3		$Pt/CeO_2/Al_2O_3$	
	Particle size (nm)	Surface area (m^2/g)	Particle size (nm)	Surface area (m^2/g)
Fresh calcined	1.4 ± 0.3	127	1.8 ± 0.4	129
H_2S poisoned	6.2 ± 1.2	111	4.9 ± 0.9	118
H_2 regenerated	5.2 ± 0.9	123	2.6 ± 0.5	111

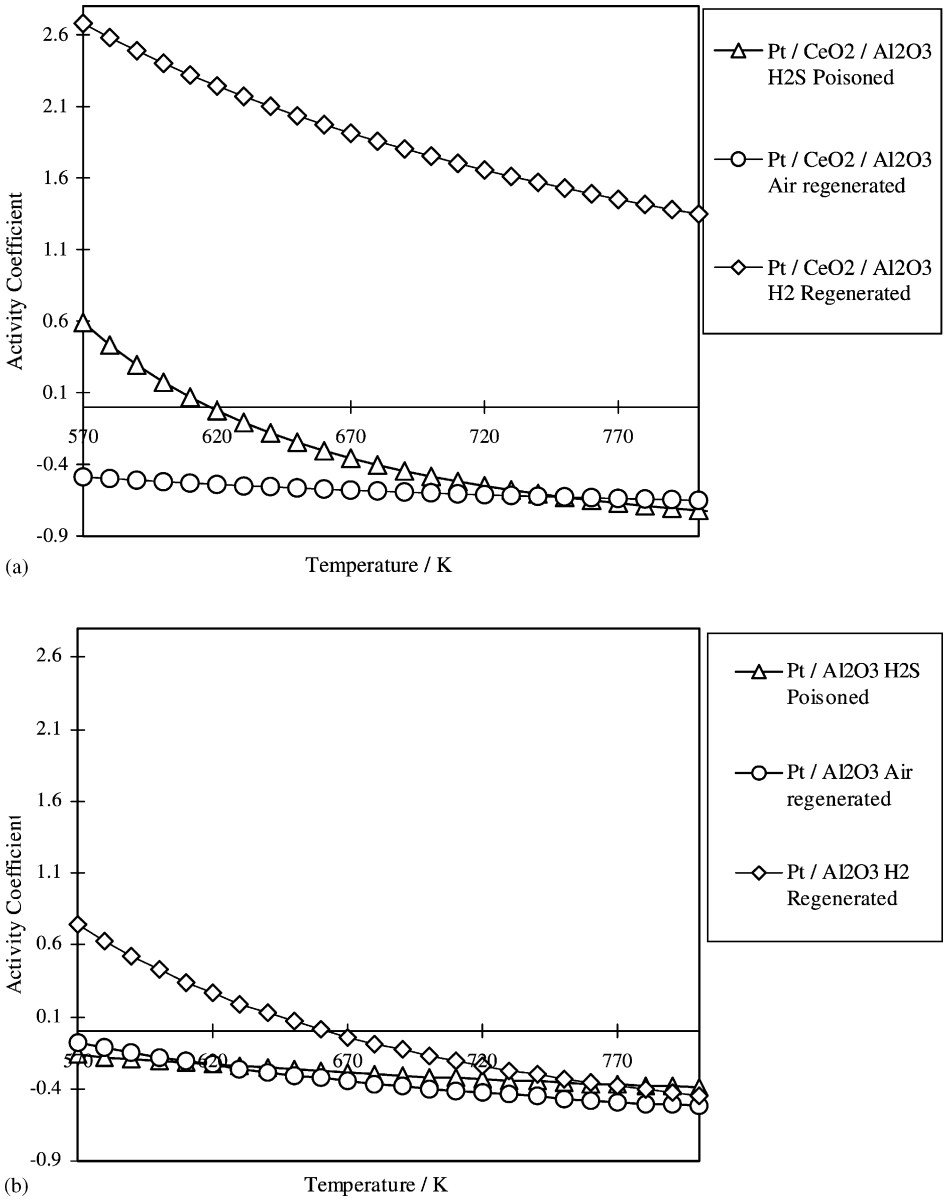

Fig. 2. Activities of: (a) $Pt/CeO_2/Al_2O_3$ and (b) Pt/Al_2O_3 expressed as ($k_{poisoned/regenerated}/k_{fresh}$) vs. T/K.

4. Discussion

4.1. Pt/Al_2O_3 (air pretreated) vs. $Pt/CeO_2/Al_2O_3$ (air pretreated)

From Fig. 1, it can be seen that the ceria–alumina-supported catalyst is more active for low temperature methane combustion than Pt/Al_2O_3. Cerium oxide is employed for the stabilisation of metal dispersion and alumina support. The success of ceria and CeO_2-based materials is mainly attributed to the unique combination of an elevated oxygen transport capacity coupled with the ability to shift easily between reduced and oxidised sates (i.e. Ce^{3+}–Ce^{4+}) [49]. This means that

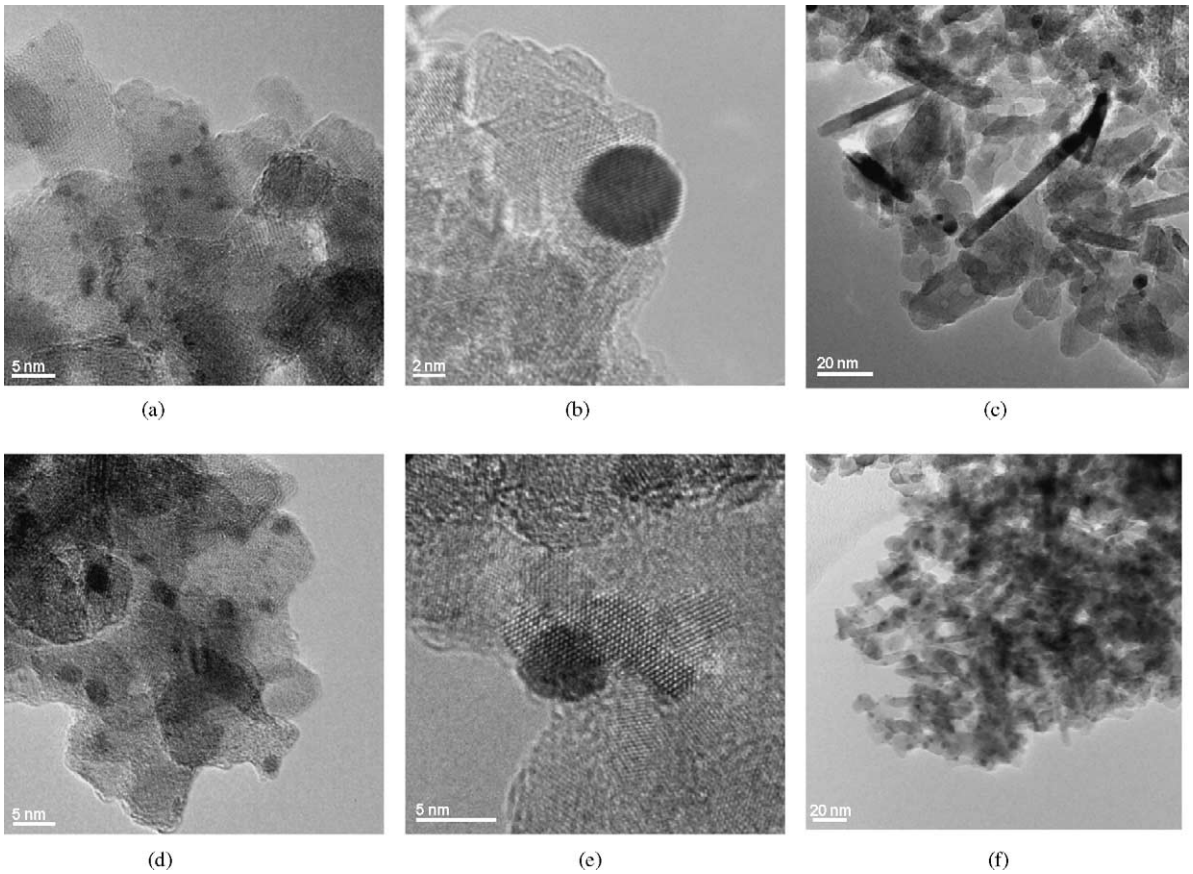

Fig. 3. TEM images of: (a) Pt/Al_2O_3 freshly calcined, (b) Pt/Al_2O_3 H_2S poisoned, (c) Pt/Al_2O_3 H_2S poisoned, (d) $Pt/CeO_2/Al_2O_3$ freshly calcined, (e) $Pt/CeO_2/Al_2O_3$ H_2S poisoned and (f) $Pt/CeO_2/Al_2O_3$ H_2S poisoned.

cerium oxide plays an important role for promoting oxygen activation and consequently an enhancement in catalytic activity. In general, catalytic combustion of methane is considered to proceed via successive steps such as the formation of active species (e.g. O^* and CH_X^* (and subsequently C^* and H^* where $*$ represents a surface species) by the dissociative adsorption of methane and oxygen [50]. The chemisorbed oxygen reacts with surface carbon and hydrogen species via:

$$C^* + O^* \rightarrow CO^*$$

$$CO^* + O^* \rightarrow CO_2(g)$$

$$H^* + O^* \rightarrow OH^*$$

$$OH^* + H^* \rightarrow H_2O(g)$$

From the reaction mechanism, it is apparent that the activation of oxygen is one of the important steps for initiating methane oxidation.

It has been reported that the novel property for oxygen activation is induced by the non-stoichiometric structure of cerium oxide, expressed in terms of CeO_{2-x}. It is proposed that methane oxidation over CeO_{2-x}/Al_2O_3 proceeds through the dissociation and diffusion of adsorbed oxygen into the vicinity of CeO_{2-x} crystallites, and then the reaction occurred between the lattice oxygen formed and methane [15]. Methane oxidation over $Pd/CeO_{2-x}/Al_2O_3$ is presumed to proceed in a similar reaction mechanism, but the presence of Pd enhances the methane oxidation even at 673 K. The reason is ascribed to the fast diffusion rate of oxygen in the lattice of CeO_{2-x}. Namely,

the lattice vacancies in CeO_{2-x} crystallites store the spillover oxygen from Pd to maintain the active palladium, and the oxygen generated from CeO_{2-x} crystallites migrates onto Pd, on which methane could be dissociated, by the reverse spillover. However, it has been proposed that the behaviour of lattice oxygens in cerium oxides differs, depending upon the structure of cerium oxide and/or the employed supports. A large amount of the lattice oxygens were desorbed easily from $Pd/CeO_{2-x}/Al_2O_3$ at 673 K, while the desorption of the lattice oxygens from $Pd/CeO_2/Al_2O_3$ and $Pd/CeO_2/SiO_2$ was not recognised [12].

Bunluesin et al. [51] compared steady-state, CO oxidation rates on ceria-supported Pt, Pd, and Rh catalysts over a wide range of temperatures and partial pressures. Large enhancements in the steady-state rates were observed on the ceria-supported catalysts, over that which would be expected from the precious metals themselves, especially for Pt at lower temperatures. The results suggest that the rates were non-specific to the metal–ceria interface and that it is the ceria properties that affect the reaction. This data supports the results obtained from the present study.

It is known that the physicochemical properties of active species such as the dispersion state and the crystallite structure are affected strongly by the preparation procedure. It is also known that there are considerable kinds of non-stoichiometric cerium oxide between CeO_2 and Ce_2O_3. The cerium oxide on CeO_2/Al_2O_3 catalysts prepared by impregnation or the sol–gel methods has been identified as the cerium dioxide (CeO_2) after oxidation. However, when reduced in a H_2 stream the cerium dioxide on the CeO_2/Al_2O_3 catalyst prepared by the impregnation method is reduced to form cerium aluminate ($CeAlO_3$), while the cerium dioxide on the CeO_2/Al_2O_3 catalyst prepared by the sol–gel method is reduced to form amorphous cerium oxide. This amorphous cerium oxide is confirmed to be many kinds of non-stoichiometric cerium oxides (CeO_{2-x}) [12].

The preparation technique used in the manufacture of the supports used in this experiment was impregnation, suggesting that upon calcination the cerium oxide would be present as the cerium dioxide (CeO_2). Although this has previously been identified as the less active form in comparison to amorphous cerium oxide, it is still clear from the results and from previous studies [51] that the level of oxygen activation is increased with the incorporation of cerium oxide into the support, based primarily on its oxygen storage capacity.

4.2. Pt/Al_2O_3 (H_2S poisoned) vs. $Pt/CeO_2/Al_2O_3$ (H_2S poisoned)

It is apparent with reference to the activity coefficients (Fig. 2) that both catalysts suffer a certain level of deactivation for methane combustion in the presence of H_2S. The overall loss of activity was more significant for the $Pt/CeO_2/Al_2O_3$ catalyst compared to Pt/Al_2O_3, but the H_2S had a smaller influence on $Pt/CeO_2/Al_2O_3$ at lower conversions (i.e. lower temperature). It is clear that there is no enhancement in the activity of the Pt/Al_2O_3 catalyst upon exposure to H_2S, although this has been previously reported [8,42]. There does appear to be a small promotional effect at low conversion levels for the $Pt/CeO_2/Al_2O_3$. Although this has not been reported before, it is important to note that that the use of activity coefficients can magnify small trends and that the results corresponding to an activity increase are at conversions below 5%.

From Fig. 1, it is clear that the $Pt/CeO_2/Al_2O_3$ catalyst displays an overall greater shift to poorer activity upon exposure to the H_2S. This observed deactivation is likely to be through the formation of sulphate species on the oxygen-storage component, as found by Hilaire et al. [47]. They examined the effect of SO_2 poisoning on Pd/Al_2O_3 and $Pd/CeO_2/Al_2O_3$ catalysts. After pre-exposure of 20 ppm SO_2 at 673 K no changes in the light-off curves for CO oxidation on Pd/Al_2O_3 was observed. The same pretreatment resulted in a significant upward shift in the light-off curves for $Pd/CeO_2/Al_2O_3$, so that the poisoned $Pd/CeO_2/Al_2O_3$ catalysts exhibited similar rates to that of Pd/Al_2O_3. These results reflect similar trends to those obtained from the present study. The conversion vs. temperature profile for $Pt/CeO_2/Al_2O_3$ poisoned, and Pt/Al_2O_3 fresh, are very similar, implying that the sulphur species may selectively react with the cerium oxide so that any benefit from cerium oxide incorporation into the support is removed.

It has been widely reported that SO_2 reacts with dispersed ceria to form a sulphate. Beck et al. found

sulphur uptake in pelleted and monolithic commercial catalysts following exposures at 773 K to cycled exhaust gas containing 20 ppm SO_2. They concluded that sulphur uptake is a surface phenomena involving only exposed Ce, some of which they attributed to sulphate [52]. Lööf et al. [25] found that exposure of Pt/ceria catalysts to excess SO_2, in excess O_2 at 773 K yielded sulphate. They concluded that the sulphate was bulk $Ce_2(SO_4)_3$ and also recognised that the simultaneous reduction of Pt under these oxidising conditions suggests that Pt catalyses the oxidation of SO_2. The resulting SO_3 may be responsible for sulphate formation, which is therefore catalysed by the presence of Pt [44].

It is likely that the deactivation observed for the $Pt/CeO_2/Al_2O_3$ is due to a significant decrease in the rate of oxygen transfer due to the presence of sulphate species. It would appear that this is not the case for the Pt/Al_2O_3 catalyst. This is very evident from the TEM images obtained from the catalyst samples (Fig. 3), and the results given in Table 2 showing that the average Pt particle size increased by over a factor of four for the Pt/Al_2O_3 catalyst upon exposure to the sulphur mixture. The level of Pt metal agglomeration in the alumina-supported catalyst was significantly greater than that of the ceria–alumina-supported catalyst. This indicates that metal migration is induced by sulphur poisoning. This was observed in a previous study by Chang et al. [41] in which the Pt–Pt first shell coordination number increased from 2.6 to 7.3, indicating the increasing size of Pt clusters. Similarly, Lee et al. observed large metallic Pt clusters upon sulphation of Pt/Al_2O_3 catalysts. They determined this was due to reduction and concomitant sintering of β-Pt/Al_2O_3 particles [53]. With increasing Pt particle size, there is a consequent loss in active surface area, resulting in a decrease in the catalytic activity. The results from Table 2 show a notable loss of surface area for the Pt/Al_2O_3 catalyst upon exposure to the H_2S mixture. It is known that sulphur species bond very strongly to the active sites of the catalysts, forming stable surface metal sulphides, thereby preventing the reactants from adsorbing at the surface. Following sulphation, Lee et al. [53] found that all Pt/Al_2O_3 samples displayed a significant loss of between 20 and 35% of their fresh surface areas consistent with the crystallisation of amorphous alumina as aluminium sulphate hydrates. The formation of sulphide is therefore very likely to be responsible for a certain degree of the loss in activity, although Pt-agglomeration and the consequent loss of active surface area are likely to be the major mechanisms of deactivation for the Pt/Al_2O_3 catalyst.

It is apparent that the $Pt/CeO_2/Al_2O_3$ catalyst does not suffer to a similar extent the level of Pt-agglomeration or loss of surface area displayed by the Pt/Al_2O_3 catalyst (Table 2). The reason for this is related to the well-known ability of ceria to stabilise the alumina support and promote noble/precious metal dispersion [11,47,54]. Clearly, although the ceria-supported catalyst suffered a greater overall level of deactivation, it was not due to a change in the structure of the support. This is important when considering that sulphation of the support is a second factor that may contribute to sulphur poisoning. Sulphation of CeO_2 or Al_2O_3 can alter the crystalline structure and nature of the support. This is expected to have an impact on the metal–support interaction. For example, in a previous study H_2S-induced catalyst poisoning of PdO/γ-Al_2O_3 was attributed to the formation of aluminium sulphate ($Al_2(SO_4)_3$) from the SO_2 and SO_3 generated from PdS oxidation [55]. Due to the formation of sulphite and sulphate, BET surface area and CO chemisorption decrease due to the occlusion of some PdO sites, leading to catalyst deactivation. There is evidence that indicates the Pt/Al_2O_3 catalyst suffered a certain degree of sulphation (Fig. 3c). The elongation of the alumina crystals (indicating a change in the support structure), in addition to the loss of surface area (Table 2) can be attributed to the effects of sulphur exposure. Sulphation may therefore possibly be a mechanism by which the Pt/Al_2O_3 catalyst was deactivated. The $Pt/CeO_2/Al_2O_3$ catalyst on the other hand showed no signs of a change in the support structure (Fig. 3f) as expected, due to its ability to stabilise the support structure. The apparent loss of surface area can be attributed to the formation of sulphate groups and to a lesser extent Pt-agglomeration.

4.3. *Pt/Al_2O_3 (air regenerated) vs. $Pt/CeO_2/Al_2O_3$ (air regenerated)*

For both catalysts air regeneration was unsuccessful. From the preceding discussion, it is apparent that sulphation of the supports contribute to catalyst

deactivation probably via $Al_2(SO_4)_3$ surface species in the case of Pt/Al_2O_3, and surface cerium sulphates in the case of $Pt/CeO_2/Al_2O_3$. Since, under oxidising conditions, surface sulphates do not begin to decompose until >600 °C, it is not surprising that this regeneration method is unsuccessful [45]. The use of higher temperatures was not explored since this can lead to severe Pt sintering [35,36].

4.4. Pt/Al_2O_3 (H_2 regenerated) vs. $Pt/CeO_2/Al_2O_3$ (H_2 regenerated)

It is clear from the results (Fig. 2) that H_2 regeneration was successful for both catalysts. This is because both surface sulphite and sulphate groups can be removed from the poisoned catalyst surface by H_2 treatment at relatively low temperatures. H_2 can convert SO_3 groups into SO_2 groups, which are more easily removed from the catalyst surface [55].

It can be seen from the results (Fig. 4a) that although the activity of the Pt/Al_2O_3 catalyst has been restored (Fig. 2), the sulphur poisoned catalyst support structure was not regenerated completely as elongated alumina crystals could still be seen. The surface structure has been restored to a certain degree, indicated by an increase in the BET surface area (Table 2). The restoration of the active surface area may also be attributed to a decrease in the average active metal particle size (Table 2), although it is clear that the effects of Pt-agglomeration are still present, just to a lesser extent (Fig. 4b and c).

The most interesting aspect of the H_2 treatment is the resulting promotion in the activity of the $Pt/CeO_2/Al_2O_3$. The activity displayed by the H_2

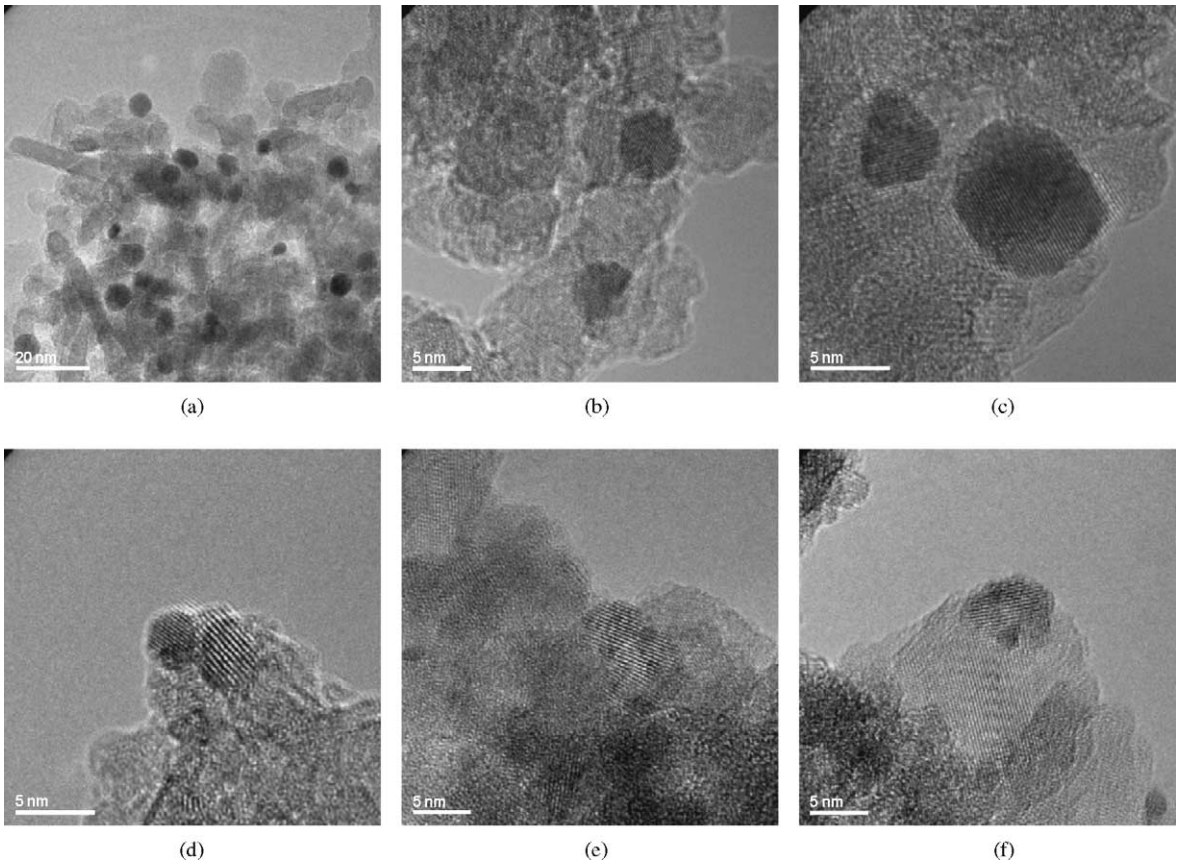

Fig. 4. TEM images of: ((a)–(c)) Pt/Al_2O_3 H_2 regenerated and ((d)–(f)) $Pt/CeO_2/Al_2O_3$ H_2 regenerated.

regenerated $Pt/CeO_2/Al_2O_3$ catalyst was substantially greater than that measured in its freshly calcined state. It has been widely reported that the activity of CeO_2 supported platinum group metal catalysts is strongly dependent on the pretreatment atmosphere.

Nunan et al. reported that the presence of ceria was beneficial for oxidation of the hydrocarbon components of a synthetic exhaust mixture, after catalyst activation in the exhaust stream. Activation was associated with in situ catalyst reduction by low levels of H_2 present [28]. In agreement with a more recent study by Tiernan and Finlayson [11], TPR profiles indicate the existence of a direct platinum group metal–CeO_2 interaction which was found to correlate with improved light-off performance after activation. It was concluded that Pt migrated selectively to CeO_2 during preparation and that direct interaction between the two metals led to dramatic improvements in catalyst light-off activity following in situ reduction. Diwell et al. [29] also proposed that an induced Pt–CeO_2 interaction occurred during reduction which greatly affected the nature and activity of the catalytic sites. TPR profiles also indicated the existence of a Pt–CeO_2 interaction upon reduction. This was proposed to involve Pt encapsulation by partially reduced CeO_2, with increased CO and NO removal being associated with the formation of ion vacancies in the support. The role of the metal particles was to act as an electron donor or sink. In agreement with this theory, Hardacre et al. found that in some cases Pt which was fully encapsulated by CeO_2 was more active than a clean Pt surface. This was attributed to enhanced conversion of CO by CeO_2, due to the interaction of the oxide with the underlying Pt [56]. For supported catalysts, it was suggested that partial encapsulation would be more favourable, allowing greater participation of Pt in the catalytic reaction.

From the results (Fig. 4c–e), it would appear that upon reduction the Pt particles become intimately associated to the cerium oxide. The cerium oxide is easily distinguished on the images as areas of clear contrast, as ceria has a higher electron density than platinum. It also has distinctive lattice spacing greater than that of platinum. A good image is Fig. 3e in which a platinum particle can be seen associated with an area of ceria upon the alumina support. This intimate association suggests the Pt particles selectively migrate towards the ceria, forming as suggested in other reports, a bimetallic interaction, increasing the activity of the catalyst. Whether or not the Pt particles become encapsulated within the cerium oxide to any extent cannot be distinguished from the TEM images.

5. Conclusions

The incorporation of cerium oxide into the support structure of Pt/Al_2O_3 catalysts is beneficial in terms of methane oxidation activity. The measured increase in activity is based primarily on the additional oxygen storage capacity offered by cerium oxide and the consequential increase in oxygen activation. Upon exposure to a sulphur poison (e.g. H_2S), it would appear that any advantage offered by cerium oxide is completely lost probably due to the formation of sulphate species on the oxygen storage component, causing a decrease in the rate of oxygen transfer. This is why the level of activity for the $Pt/CeO_2/Al_2O_3$ deactivated to that of the fresh Pt/Al_2O_3 catalyst. It did not deactivate to the same level as the poisoned Pt/Al_2O_3 catalyst as the additional benefits of ceria, the increased support stability and promoted precious metal dispersion, prevented any further deactivation. The mechanisms of deactivation for the alumina-supported catalyst are different to those of the ceria–alumina-supported catalyst as Pt-agglomeration and surface sulphation seem to play a greater role.

It would appear that as previously reported, pretreatment plays an important role in the activity of ceria-supported platinum group metal catalysts. A reductive pretreatment is required to induce the platinum group metal–CeO_2 interaction and activate the catalyst to its full potential. This is why the activity measured for the $Pt/CeO_2/Al_2O_3$ catalyst after H_2 treatment surpassed that of the freshly calcined catalyst.

Acknowledgements

The authors are grateful to JM for preparing the catalysts, and iAc and EPSRC are gratefully acknowledged for financial support in the form of a studentship. The authors also thank Andy Brown for help with the TEM work.

References

[1] S.R. Vatcha, Energy Conv. Manage. 38 (10–13) (1997) 1327.
[2] S. Cimino, L. Lisi, R. Pirone, G. Russo, M. Turco, Catal. Today 59 (2000) 19.
[3] K. Sekizawa, H. Widjaja, S. Maeda, Y. Ozawa, K. Eguchi, Catal. Today 59 (2000) 69.
[4] T.V. Choudhary, S. Banerjee, V.R. Choudhary, Appl. Catal. A 234 (2002) 1.
[5] P. Euzen, J. Le Gal, B. Rebours, G. Martin, Catal. Today 47 (1999) 19.
[6] H. Widjaja, K. Sekizawa, K. Eguchi, H. Arai, Catal. Today 35 (1997) 197.
[7] K. Sekizawa, K. Eguchi, H. Widjaja, M. Machida, H. Arai, Catal. Today 28 (1996) 245.
[8] J.H. Lee, D.L. Trimm, Fuel Process. Technol. 42 (1995) 339.
[9] S. Imamura, T. Yamashita, R. Hamada, Y. Saito, Y. Nakao, N. Tsuda, C. Kaito, J. Mol. Catal. A 129 (1998) 249.
[10] A. Cook, A.G. Fitzgerald, J.A. Cairns, Catalysis and Surface Characterisation, Royal Society of Chemistry, Cambridge, 1992, p. 249.
[11] M.J. Tiernan, O.E. Finlayson, Appl. Catal. B 19 (1998) 23.
[12] M. Haneda, T. Mizushima, N. Kakuta, J. Phys. Chem. B 102 (1998) 6579.
[13] M. Ozawa, M. Kimura, J. Mater. Sci. Lett. 9 (1990) 291.
[14] K.J. Blackenburg, A.K. Datye, J. Catal. 128 (1991) 1.
[15] M. Haneda, T. Mizushima, N. Kakuta, J. Chem. Soc., Faraday Trans. 91 (1995) 4459.
[16] M. Haneda, T. Mizushima, N. Kakuta, A. Ueno, Y. Sato, S. Matsuura, K. Kasahara, M. Sato, Bull. Chem. Soc. Jpn. 66 (1993) 1279.
[17] M. O'Connell, M.A. Morris, Catal. Today 59 (2000) 387.
[18] G. Groppi, C. Cristiani, L. Lietti, C. Ramella, M. Valentini, P. Forzatti, Catal. Today 50 (1999) 399.
[19] M. Haneda, T. Mizushima, N. Kakuta, A. Ueno, Bull. Chem. Soc. Jpn. 67 (1994) 2617.
[20] Y.Q. Deng, T.G. Nevell, Faraday Discuss. 105 (1996) 33.
[21] Y.Q. Deng, T.G. Nevell, Catal. Today 47 (1999) 279.
[22] J.C. Summers, S.A. Ausen, J. Catal. 58 (1979) 131.
[23] Y.F. Yu-Yao, J.T. Kummer, J. Catal. 106 (1987) 307.
[24] S.H. Oh, C.C. Eickel, J. Catal. 112 (1988) 543.
[25] P. Lööf, B. Kasemo, L. Björnkvist, S. Andersson, A. Frestad, Catalysis and automotive pollution control II, Stud. Surf. Sci. Catal. 71 (1991) 253.
[26] C. Serre, F. Garin, G. Belot, G. Maire, J. Catal. 48 (1989) 71.
[27] B. Engler, E. Koberstein, P. Schubert, Appl. Catal. 48 (1989) 71.
[28] J.G. Nunan, H.J. Robota, M.J. Cohn, S.A. Bradley, J. Catal. 133 (1992) 309.
[29] A.F. Diwell, R.R. Rajaram, H.A. Shaw, T.J. Truex, Catalysis and automotive pollution control II, Stud. Surf. Sci. Catal. 71 (1991) 139.
[30] Y.F. Yu-Yao, Ind. Eng. Chem. Prod. Res. Dev. 19 (1980) 293.
[31] H.S. Gandhi, M. Shelef, Catalysis and automotive pollution control II, Stud. Surf. Sci. Catal. 30 (1987) 199.
[32] L. Prilaut, D. El Azami El Idrissi, P. Marecot, J.M. Dominguez, G. Mabilon, M. Prigent, J. Barbier, Catalysis and automotive pollution control II, Stud. Surf. Sci. Catal. 96 (1995) 193.
[33] J.T. Kummer, Y.F. Yu-Yao, D. McKee, Proceedings of the American Engineering Congress, Detroit, MI, 1976 (Abstr. No. 760143).
[34] S.H. Oh, P.J. Mitchell, R.M. Siewert, J. Catal. 132 (1991) 287.
[35] J.A. Moulijn, A.E. van Diepen, F. Kapteijn, Appl. Catal. A 212 (2001) 3.
[36] C.H. Bartholomew, Appl. Catal. A 212 (2001) 17.
[37] P. Reyes, G. Pecchi, M. Morales, J.L.G. Fierro, Appl. Catal. A 163 (1997) 145.
[38] Z. Paál, K. Matusek, M. Muhler, Appl. Catal. A 149 (1997) 113.
[39] V. Meeyoo, D.L. Trimm, N.W. Cant, Appl. Catal. B 16 (1998) L101.
[40] N.S. Shawal, J.M. Jones, V.A. Dupont, A. Williams, Energy Fuels 12 (1998) 1130.
[41] J.R. Chang, S.L. Chang, T.B. Lin, J. Catal. 169 (1997) 338.
[42] P. Reyes, G. Pecchi, Moportus, J.L.G. Fierro, Bull. Soc. Chilena Quim. 41 (1996) 173.
[43] B.I. Whittington, C.J. Jiang, D.L. Trimm, Catal. Today 41 (1994) 45.
[44] S.H. Overbury, D.R. Mullins, D.R. Huntley, L. Kundakovic, J. Phys. Chem. B 103 (1999) 11308.
[45] M. Waqif, P. Bazin, O. Saur, J.C. Lavalley, G. Blanchard, O. Touret, Appl. Catal. B 11 (1997) 193.
[46] H.N. Rabinowitz, S.J. Tauster, R.M. Heck, Appl. Catal. 212 (2001) 215.
[47] S. Hilaire, S. Sharma, R.J. Gorte, J.M. Vohs, H.W. Jen, Catal. Lett. 70 (2000) 131.
[48] J.M. Jones, V.A. Dupont, R. Brydson, D.J. Fullerton, N.S. Nasri, A.B. Ross, A.V.K. Westwood, Sulphur poisoning and regeneration of precious metal catalysed methane combustion, Catal. Today 81 (2003) 589.
[49] A. Trovarelli, M. Boara, E. Rocchini, C. Leitenburg, G. Dolcetti, J. Alloys Comp. 323–324 (2001) 584.
[50] O. Deutschmann, L.D. Schmidt, Proceedings of the 27th International Symposium on Combustion, The Combustion Institute, 1998, p. 2283.
[51] T. Bunluesin, E.S. Putna, R.J. Gorte, Catal. Lett. 41 (1996) 1.
[52] D.D. Beck, M.H. Krueger, D.R. Monroe, SAE Technical Paper 910844, 1991.
[53] A.F. Lee, K. Wilson, R.M. Lambert, C.P. Hubbard, R.G. Hurley, R.W. McCabe, H.S. Gandhi, J. Catal. 184 (1999) 491.
[54] J. Kašpar, P. Fornasiero, M. Graziani, Catal. Today 50 (1999) 285.
[55] T.C. Yu, H. Shaw, Appl. Catal. B 18 (1998) 105.
[56] C. Hardacre, R.M. Ormerod, R.M. Lambert, J. Phys. Chem. 98 (1994) 10901.